Analysis of Knee-Ankle Orthosis Modelling: An Inverse Dynamics Approach Using Adaptive Coupled Oscillator

Michael Oluwatosin Ajayi[1,2], Karim Djouani[1,2], and Yskandar Hamam[1,3]

[1] Department of Electrical Engineering, Tshwane University of Technology, Staatsartillerie Road, Pretoria West, Pretoria, South-Africa
[2] University of Paris Est Creteil (UPEC), LISSI, 94400 Vitry Sur Seine, France
[3] LISV, Btiment Boucher, Pole scientifique et technologique de Velizy, 10-12 avenue de l'Europe, 78140 Velizy
{ajayimo,djouanik,hamama}@tut.ac.za

Abstract. In this paper, an inverse dynamics approach by means of adaptive coupled oscillators is used in the modelling and control of a lower limb orthosis applied at the knee and ankle joint level. This design is aimed at providing assistance and rehabilitative measures to humans with lower limb disorders and as such presents a platform for which their mobility performance can be improved. Adaptive oscillators are known to have the capability of learning high level parameters of sinusoidal, quasi-sinusoidal or non-sinusoidal signals (amplitude, frequency and offset). However, the later signal (non-sinusoidal) considered in this paper requires a number of oscillators in parallel to replicate the moving joint regarding filtering via adaptive oscillator. The dynamic model for the knee and ankle are considered to take the form of a damped pendulum model connected by two revolute joints. This maps the input torque of both joints (knee and ankle) to their output trajectories, hence integrating the different forces at the joint level of the different joints. The coupling effect is achieved by the use of coupled Adaptive Frequency Oscillator (AFO) for the estimation of the joint trajectories. Tracking performance for the knee-ankle orthosis is studied for non-sinusoidal reference trajectories, having a global coupling between the joints. The results obtained using SCILAB show a good performance of the controller trajectory tracking capabilities even in the presence of external disturbances.

Keywords: Adaptive Coupled Oscillators, Knee-Ankle Orthosis, Rehabilitation Robotics, Robot-assisted platform.

1 Introduction

The objective of rehabilitation is to perform specific movements that exercise and hence improve motor unit plasticity of the patient thereby influencing motor recovery and minimising functional deficits [1]. Rehabilitation therefore could

D. Brugali et al. (Eds.): SIMPAR 2014, LNAI 8810, pp. 122–133, 2014.

be implemented manually or robotically (i.e. by the use of a robotic tool). Rehabilitation robotics is a branch of robotics which provides a platform for the design of robots in the form of orthosis for the purpose of providing physiotherapy to persons with physical disability. Conventional manual rehabilitation is associated with excessive time, energy and resources (physiotherapist) hence disadvantageous compared to robotic-based rehabilitation [2]. Research on the efficiency of robotic therapy has shown that rehabilitation technologies provide new alternatives for repetitive training sessions that can increase efforts to improve the therapy performance. This is also intended to reduce the burden on physiotherapists and assess quantitatively the level of motor recovery by measuring force and movement patterns [1],[3].

Robotic therapy may be performed on *traditional robotic platforms or robot-assisted platforms* [4]. The former is basically used to drive the patients limb along a pre-specified trajectory using stiff position control as in [5], thereby making the patient passive during the whole training sessions. Although this proved to be a drawback, [2] addressed the possibility for traditional robotic platforms to work in passive and active mode, depending on the recovery stage of the patients.

The "assistance-as-needed" approach as known as the robot-assisted platform helps provide assistance for movement to subjects when they are incapable of completing the movement task [6]. This allows patients to be active during the entire physiotherapy session and assisted only when required, thereby improving the patients muscle activity [7]. In [4], a novel assistance method was proposed for rhythmic movement of the forearm about the elbow using a single adaptive oscillator. The features associated with this method commensurate with that of EMG-based assistive device [8], since its level of assistance is same at steady-state for the subject and virtually no pre-specified trajectory is needed. The objective of this paper is to investigate a rehabilitation protocol method using CPGs (Central pattern generators) to perform rhythmic movements of the lower limb about the knee and ankle. Mechanical coupling about these joints are assumed to be governed by the principle behind the double pendulum dynamic behaviour. This is based on an inverse dynamic approach hence, an estimate of the torques applied to both joints is calculated and the assistance provided to the joints is a feedback of a fraction of the said calculated torques.

CPGs are biological neural networks that produce coordinated multidimensional rhythmic signals, under the control of simple input signals. The building block for the construction of the CPG in this paper is the Adaptive Frequency Oscillator (AFO) developed in [9]. In [10], a variety of different application of the AFO was highlighted. The global problem associated with estimating derivatives of noisy position signal in robotics was addressed in [11]. It thus, proposed a new approach to estimating velocity and acceleration of cyclical/periodic signals using AFOs. Application to biped locomotion control was presented in [12] hereby demonstrating how online learning and modulation of pre-recorded walking trajectories using CPGs limit cycle properties can be achieved. [13] addressed the future of humanoid robots in areas relating to performing periodic tasks. Coupled

nonlinear oscillators were used to design CPGs similar to human gait pattern applied in the locomotion of bipedal robot was exploited in [14]. An oscillator-based model-free approach designed for the assistance and rehabilitation protocols as regard walking was also demonstrated in [15].

The main contribution of this paper is to demonstrate the possibility of assisting and rehabilitating patients with both knee and ankle anomalies so as to recuperate their motor functions concurrently using CPGs. Thus, a 2 (two) DOF (degree of freedom) is considered for the knee-ankle orthotic device.

The rest of the paper is organised as follows: Section 2 presents the knee-ankle orthosis system. Section 3 gives the methodology for design of the CPG. The mathematical model of the knee-ankle orthosis is given in Section 4. Section 5 provides the simulation and results of the movement assistance of the knee-ankle joints based on certain physiological parameters. Finally, in Section 6, further work and conclusion is made.

2 Knee-Ankle Orthosis System

In this study, the authors consider a Shank-Foot CAD model as shown in Fig.1 which depicts the knee-ankle orthosis. The CAD model is assumed to incorporate the parameters of the orthosis and the users lower limb (knee and ankle to be precise). The model thus takes into account the flexion/extension of the knee about the revolute joint a and the plantar-flexion/dorsal-flexion of the ankle about b, assuming the motions are performed in a sagittal plane with the subject in a sitting position, hence the mass of the subject's shank and foot link of a single leg are those accounted for in this model. The movements of the knee-ankle orthosis are in the range $0rad \leq \theta \leq 2.35rad$ for the knee and $0rad \leq \theta \leq 0.87rad$ for the ankle. Where 0rad relates to the full knee extension, 2.35rad is the maximum flexion of the knee and $1.57rad$ corresponds to the rest position of the knee. Furthermore, $0rad$ as regard the ankle movements corresponds to the rest position of the ankle, $0.35rad$ is the maximal ankle dorsal-flexion, while $0.87rad$ denotes the maximal ankle plantar-flexion. The assisted joint positions are required to be measured, so as to determine the human torques required. It should be noted that the system is considered to reflect a controlled movement about its axis and hence seen perform a periodic motion of each link about its pivot. Having known that the system is mechanical coupled via the joints, the movement are said to be coupled and thus achieved by CPG (Adaptive Oscillators) as disscused in section 4.2. This is done to guarantee a global movement since the dynamic model of the shank-foot is treated as a decoupled system. Based on this, the periodic motions is said to assume the dynamics of a damped simple pendulum for each link.

3 CPG Design

This section describes the model of the CPG that is used to provide assistance to the knee-ankle orthosis. The design of the CPG using adaptive oscillators and

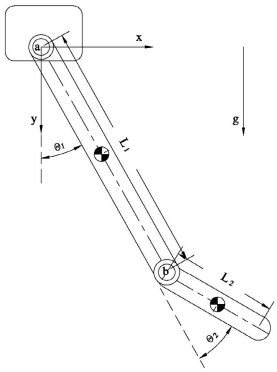

Fig. 1. Shank-Foot model

hence the tuning of the adaptive oscillator for filtering of a two (2) degree of freedom (DOF) along a non-sinusoidal trajectory are explained.

3.1 Adaptive Frequency Oscillator (AFO)

The adaptive frequency Hopf oscillator was first developed in [9] and [10]. For the purpose of simplicity, the augmented phase oscillator explained in [15] and [16] is adopted for the design of the CPGs used for the rhythmic movements needed to be achieved in this paper. The augmented phase oscillator is written as:

$$\begin{aligned} \dot{\phi} &= \omega + \nu F cos\phi \\ \dot{\omega} &= \nu F cos\phi \end{aligned} \tag{1}$$

where ϕ is the phase of the oscillator and ν represents the learning parameter that determines the speed of the phase synchronization to F and must be greater than 0; $\nu \gg 0$. F is the is the periodic input signal to which the oscillator will adapt its frequency while ω controls the frequency of the oscillations, and this is the frequency adapted to the periodic input signal F.

3.2 Coupled AFO

The idea relating to coupled oscillator was used to define a precise way of learning any periodic input signal. This was in particular used to learn non-sinusoidal periodic signals due to the fact that most human movements are not usually sinusoidal. This coupling scheme which is more than just a dynamic Fourier series decomposition of non-sinusoidal periodic signal, was first proposed in [12] and later modified using augmented phase oscillator in [15], as shown below:

$$\begin{aligned}
\dot{\phi}_i &= i\omega + \nu F cos\phi_i \\
\dot{\omega} &= \nu F cos\phi_1 \\
\dot{\alpha}_i &= \eta F sin\phi_i \\
F &= \theta - \hat{\theta} \\
\hat{\theta} &= \sum_{i=0}^{N} \alpha_i sin\phi_i
\end{aligned} \tag{2}$$

where i represents the no. of oscillators in parallel as regard the non-sinusoidal periodic signal and N the total number of oscillators. α_i is the amplitude associated to the main frequency ω, F is the is the periodic input signal to which the oscillator will adapt its frequency while θ signifies the non-sinusoidal periodic signal. $\hat{\theta}$ is the sum of filtered outputs of each oscillator and η is the amplitude integrator gain. Note that only the main frequency ω will learned to F.

Furthermore, the CPG corresponds to one degree of freedom (DOF), therefore, for 2 DOF based on the knee-ankle orthosis 2 CPGs are required. 3 oscillators relate to one CPG. This is in conjunction with the assumed non-sinusoidal trajectories of the knee and ankle respectively. Consequently, in this model, $i = 3$.

4 Mathematical Model

In this section, the building blocks for the entire system are described. The blocks include: the dynamic model, coupled AFO (which includes the signal estimator and the torque estimator) and the human torque. Fig. 2 shows the block diagram of the combined system (human knee and ankle + orthosis).

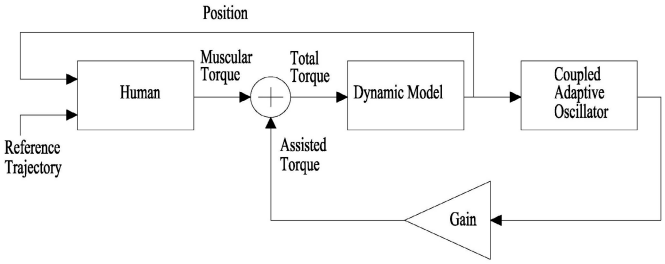

Fig. 2. Block diagram of the human knee and ankle + orthosis

4.1 Dynamic Model

The knee and ankle rhythmic movement of the human lower limb generates two trajectories and therefore the system is modelled as two (2) degree of freedom (DOF). These rhythmic movements are characterised as movements similar to that of a damped pendulum dynamics. The purpose of this has been explained

in section 2. Hence the dynamic model for the knee and the ankle can be mathematically written as:

$$\ddot{\theta_j} = {I_j}^{-1}\left(-m_j g l_j sin\theta_j - b_j\dot{\theta_j} + \tau_j\right) \tag{3}$$

with j is the number of joints which corresponds to two (2) for this particular model with $j = 1$ relating to the knee and $j = 2$ relating to the ankle and I_j symbolises the inertia of the shank/foot. m_j is the mass of the shank/foot, l_j is the equivalent length of the shank/foot, which corresponds to the movement about the knee and ankle joint while b_j represents the damping constants of the shank/foot movement about knee/ankle joints. g signifies the gravitational force, $\ddot{\theta_j}$, $\dot{\theta_j}$, θ_j denotes the knee/ankle angular acceleration, velocity and position respectively and τ_j is the total torques applied to the knee and ankle respectively. The dynamic model block simply retrieves the actual angular position by integrating (3) in relation to each joint level. The generalised coordinate which represent the actual angular position for the knee and ankle can therefore be represented as:

$$\theta = \begin{bmatrix}\theta_1 \ \theta_2\end{bmatrix}^T \tag{4}$$

4.2 Coupled AFO (Joints Coupling)

The coupling of adaptive frequency oscillators to reproduce non-sinusoidal periodic signal for a single joint was explained in Section 3.2. However, the simultaneous rhythmic movement of the knee and ankle joints requires coupling between each CPG which represent each joint. The choice of coupling used could differ, as demonstrated in [12] and [15] respectively.

This paper adapts the global coupling procedures which require a common variable belonging to each CPG controlled by each CPG. Fig. 3 presents a pictorial diagram of the coupling of the CPG with the frequency being the common variable needed to be controlled. The equation of the CPG which incorporates the global coupling between each joint can be written as:

$$\begin{aligned}\dot{\phi_i} &= i\omega + \nu F_j cos\phi_i \\ \dot{\omega} &= \left(\nu \sum_{j=1}^{G} F_j cos\phi_{1,j}\right) \diagup G \\ \dot{\alpha_i} &= \eta F sin\phi_i\end{aligned} \tag{5}$$

with j represents the active joint in question; for which in this particular model $j = 1$ relates to the knee, while $j = 2$ relates to the ankle. F_j is the non-sinusoidal periodic signal for each CPG and can be written as $F = \begin{bmatrix}F_1 \ F_2\end{bmatrix}^T$ and ω signifies the frequency and thus initiates the coupling between each CPG. G is the total number of joints while other terms are same as defined in (2).

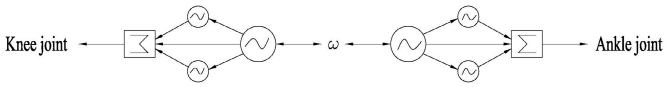

Fig. 3. Structure of CPG coupling

4.3 Signal Estimator

The non-sinusoidal input signal F_j of the adaptive oscillator is the difference between the knee-ankle angular positions θ_j and the estimated (learned) signal $\hat{\theta}_j$. This can be expressed as below:

$$\begin{aligned} F &= \theta_j - \hat{\theta}_j \\ \hat{\theta}_j &= \sum_{i=0}^{K} \alpha_{i,j}\, sin\phi_{i,j} \end{aligned} \tag{6}$$

The adaptive oscillator estimate of the velocity and acceleration can be written respectively as in [16]:

$$\begin{aligned} \dot{\hat{\theta}}_j &= \sum_{i=0}^{K} \alpha_{i,j}\, \omega cos\phi_{i,j} \\ \ddot{\hat{\theta}}_j &= -\left(\sum_{i=0}^{K} \alpha_{i,j}\, \omega^2 sin\phi_{i,j} \right) \end{aligned} \tag{7}$$

4.4 Torque Estimator

The estimated torques is derived from the dynamic model in (3). The value of which is obtained by introducing the estimates from the adaptive oscillators described in (6) & (7). This forms the basis of the AFO control system. The equation may be described as:

$$\hat{\tau_j} = m_j g l_j sin\hat{\theta}_j - b_j \dot{\hat{\theta}}_j + I_j \ddot{\hat{\theta}}_j \tag{8}$$

with each symbol defined as in section 4.1 but represents its estimated version.

4.5 Human Torque

The human (muscular) torque applied to the device is determined by the PID controller in conjunction with the reference trajectory for the purpose of simulation and it is thus defined as:

$$\tau_{h,j} = K_{p,j}\, e_j + K_{i,j} \int e_j dt + K_{d,j}\, \dot{e_j} \tag{9}$$

where e_j is the error signal which is the difference between the reference trajectories and actual angular positions of the knee/ankle and $K_{p,j}$, $K_{i,j}$, $K_{d,j}$ are the proportional, integral and derivative gains of the controller (human torque) about the knee/ankle.

The total torque τ_j is the sum of the human (muscular) torque $\tau_{h,j}$ and the assistive torque $\tau_{e,j}$:

$$\tau_j = \tau_{h,j} + \tau_{e,j} \tag{10}$$

with $\tau_{e,j} = \kappa_j \hat{\tau_j}$ where κ_j determines the level of assistance applied at the knee/ankle joint. $\kappa_j = 1$ implies full assistance, $\kappa_j = 0.5$ represents 50% assistance and $\kappa_j = 0$ signifies no assistance.

5 Numerical Simulation

In this section, the physiological parameters, the non-sinusoidal periodic reference trajectories chosen for the purpose of this simulation and the eventual results of the simulation are highlighted.

5.1 Reference Trajectories and Physiological Parameters

The reference trajectories are assumed to be the measured angular position of the knee and ankle and chosen to be within the range of motion specified in section 2; they are given as below respectively:

$$\begin{aligned} \theta_{ref_1} &= \tfrac{\pi}{12}(sin(2\pi ft) + 0.5cos(\pi ft) + 2.25sin(\tfrac{\pi}{2}ft)) \\ \theta_{ref_2} &= \tfrac{\pi}{90}(sin(\pi ft) + 0.8cos(\tfrac{\pi}{2}ft) + 0.6sin(\tfrac{\pi}{4}ft)) \end{aligned} \tag{11}$$

with $f = 0.16Hz$

Furthermore, the physiological parameters of the knee/ankle with respect to the Shank-Foot Model in Fig. 1. were chosen as in Table: 1. below:

Table 1. Physiological Parameters

Parameters	Units	Values
Shank length (L_1)	m	0.2
Foot length (L_2)	m	0.08
Shank mass (m_1)	kg	2.80
Foot mass (m_2)	kg	1.17
Shank inertia (I_1)	$kg.m^2$	0.075
Foot inertia (I_2)	$kg.m^2$	0.012
gravity (g)	m/s^2	9.8
Shank damping Coeffiecient b_1	Nm/s^2	0.4
Foot damping Coeffiecient b_2	Nm/s^2	0.6

Note that the value of the inertia is calculated assuming cylindrical links and thus calculated as $I_i = \frac{2}{3} m_i {L_i}^2$.

The PID controller parameters and Adaptive Oscillator parameters are given as; $K_p = 110, K_i = 5.5, K_d = 2$ are same for both knee and ankle PID controllers and the adaptive oscillator parameters values $\eta = 5, \nu = 25$ are the same for each CPG representing the knee or ankle.

5.2 Results

With regards to Section 5.1, the simulation results are given in the figures below.

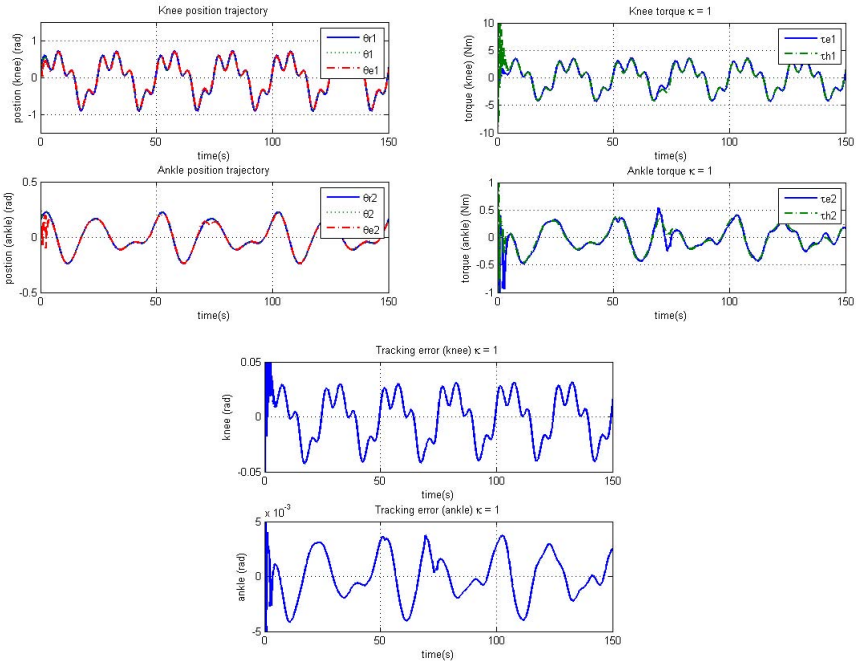

Fig. 4. Top (left): Position trajectory of knee and ankle with adaptive oscillator synchronisation. $\theta_{r1}, \theta_1 \& \theta_{e1}$ represents the reference, actual and estimated angular position trajectories of the knee respectively, while $\theta_{r2}, \theta_1 \& \theta_{e2}$ signifies the reference, actual and estimated angular position trajectories of the ankle in the same other. This same for the top figure in Fig. 6. **Top (right)**: Human (muscular) torque and assistive torque simulation of knee and ankle $\kappa = 1$. $\tau_{e1} \& \tau_{h1}$ defines the assistive torque and human torque for the knee respectively while $\tau_{e2} \& \tau_{h2}$ is same as regard the ankle. This same for Fig. 5 (torque figures only), but with different assistive torques. **Bottom**: Tracking error result of knee and ankle with adaptive oscillator synchronisation. This is a measure of how close the assistive torque follows the human torque of which it is benchmarked, based on the difference between the actual trajectory and the reference trajectory.

5.3 Discussion

As shown in Fig. 4 (top (right)) the adaptive oscillator was able to achieve phase synchronization of all three trajectories which includes the reference, actual and estimated angular positions (knee and ankle). A considerable replication of the reference trajectories was achieved with little finite time convergence of for both positions. This is true for all the conditions which vary from $\kappa = 1$ (full assistance), $\kappa = 0.5$ (50 % assistance) and $\kappa = 0$ (no assistance). By observing Fig. 4

(bottom), the tracking errors for the angular positions (knee and ankle) are relatively small with RMS errors value of $0.01012rad$ for the knee position and $0.00308rad$ for the ankle position.

In Fig.4 (top (right)) and Fig.5 (top (left) & top (right)), the level of assistance offered to the subject and the human torque of the subject is plotted with time. This is to verify the effect of the assistance to the subject during a particular training session. It can be perceived from these figures that as the level of assistance decreases from $\kappa = 1$ to $\kappa = 0$, the human torque required to achieve the proposed task increases. The orthotic device can therefore fully or partially assist the patient bringing into to play the term "assist as needed".

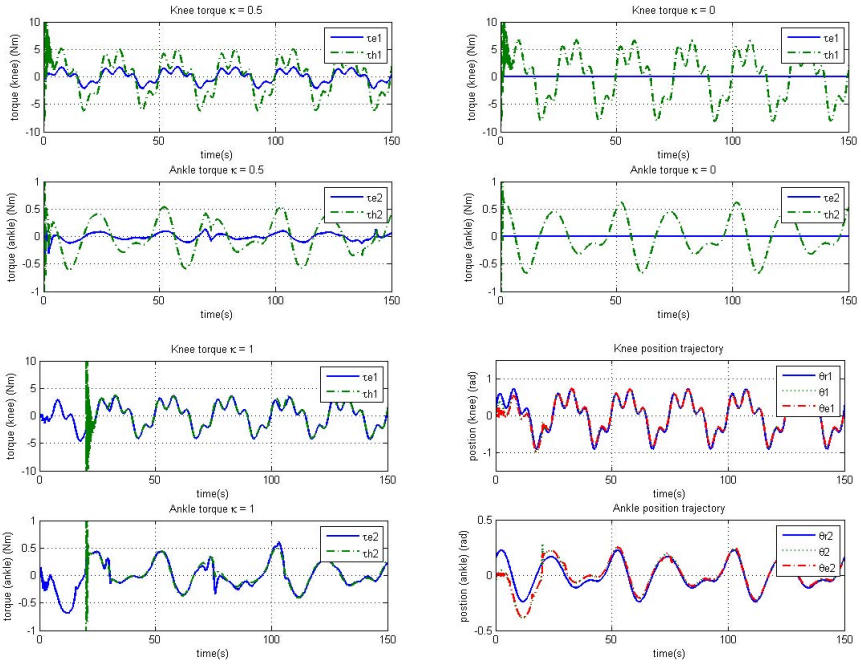

Fig. 5. Top (left): Human (muscular) torque and assistive torque simulation of knee and ankle $\kappa = 0.5$. **Top (right):** Human (muscular) torque and assistive torque simulation of knee and ankle $\kappa = 0$. **Bottom (left)**: Human and assistive torque simulation of knee and ankle $\kappa = 1$ with disturbance. It shows the interval of applied disturbance in human torque which is between $0 - 20s$. **Bottom (right)**: Position trajectory of knee and ankle with adaptive oscillator synchronisation in the presence of disturbance.

To further authenticate the assistive measures rendered, a disturbance which exemplifies the state of inactivity of the human muscles about the knee and ankle was introduced to the knee-ankle orthotic device (system). Its introduction is at early phase of the training session with full assistive measure to compensate for this muscle inactiveness (i.e. at $0 - 20s$). In real-life circumstances, it could be viewed as an abstruction to the movement of the shank-foot during the training session.

A significant ripple effect on the trajectories of the positions was observed in Fig. 5 (bottom (right)) at the early stage but all the trajectories achieved phase synchronisation at the end of stipulated training session time. This was due to the full assistance given to the subject by the device. Fig. 5 (bottom (left)) virtually demonstrates this effect; having observed that the human torque was abnormal or ineffective between $0-20s$, and the effect could be perceived in Fig. 5 (bottom (right)), due to the tracking dificulties encountered as a result of the disturbance.

Initial spikes of the PID controller which generates the human torques can be seen in figures which describes the said torque pattern. This can be eliminated by tuning the PID parameters more efficiently. However, this is for simulation purpose only as the practical use will be to measure the angular position of the periodic motions of the shank and foot about the knee and ankle respectively. This parameter is then used to calculated the human torques in conjuction with the eventual assistive torques via the estimation of the position, velocity and acceleration by the AFO.

The main contribution is to establish a rehabilitation protocol which incorporates the knee and ankle using the *robotic-assisted platform* by means of the AFO and that has been achieved based on the above simulations.

6 Conclusions and Future Works

In this paper, an assistive method for the knee and ankle rehabilitation was proposed. This was achieved by exploiting the rhythmic traits of CPGs (adaptive frequency oscillators) for the purpose of developing a new rehabilitation protocol that requires the knee and ankle concurrent movement with the aid of a global coupling. An inverse dynamic model assumed to be a simple damped pendulum dynamics for each link was used to realise a conceived movement pattern. Using a chosen numerical data, the assistive orthotic device was confirmed to be effective. This was established by mimicking the muscular (human) torque with the aid of a PID controller.

In future works, the authors intend to verify this assistive effect in a lab and also carry out parametric identification by the use of least square method and regression equations of Zatsiorsky [17] which will be achieved by sampling the inverse dynamic model along stipulated trajectories of both the knee and ankle [18]. Furthermore, the final goal will be to implement this control method to specific human gait systems using its inverse dynamic model.

References

1. Iaki, D., Jorge, J.G., Emilio, S.: Lower-Limb Robotic Rehabilitation: Literature Review and Challenges. Journal of Robotics (2011)
2. Kordasz, M., Kuczkowski, K., Sauer, P.: Study on possible control algorithms for lower limb rehabilitation system. In: IEEE International Conference on Rehabilitation Robotics (ICORR), pp. 1–6 (2011)

3. Dollar, A.M., Herr, H.: Lower Extremity Exoskeletons and Active Orthoses: Challenges and State-of-the-Art. IEEE Transactions on Robotics 24, 144–158 (2008)
4. Ronsse, R., Vitiello, N., Lenzi, T., van den Kieboom, J., Carrozza, M.C., Ijspeert, A.J.: Adaptive oscillators with human-in-the-loop: Proof of concept for assistance and rehabilitation. In: 3rd IEEE RAS and EMBS International Conference on Biomedical Robotics and Biomechatronics (BioRob), pp. 668–674 (2010)
5. Colombo, G., Wirz, M., Dietz, V.: Driven gait orthosis for improvement of locomotor training in paraplegic patients. Spinal Cord 39 (2001)
6. Wolbrecht, E.T., Chan, V., Reinkensmeyer, D.J., Bobrow, J.E.: Optimizing Compliant. Model-Based Robotic Assistance to Promote Neurorehabilitation. IEEE Transactions on Neural Systems and Rehabilitation Engineering 16, 286–297 (2008)
7. Israel, J.F., Campbell, D.D., Kahn, J.H., Hornby, T.G.: Metabolic Costs and Muscle Activity Patterns During Robotic- and Therapist-Assisted Treadmill Walking in Individuals With Incomplete Spinal Cord Injury. Physical Therapy 86, 1466–1478 (2006)
8. Sankai, Y.: Leading edge of cybernics: Robot suit hal. In: International Joint Conference SICE-ICASE, pp. P-1–P-2 (2006)
9. Righetti, L., Buchli, J., Ijspeert, A.J.: From dynamic hebbian learning for oscillators to adaptive central pattern generators. In: Proceedings of 3rd International Symposium on Adaptive Motion in Animals and Machines, AMAM, p. 45 (2005)
10. Righetti, L., Buchli, J., Ijspeert, A.J.: Adaptive frequency oscillators and applications. Open Cybernetics and Systemics Journal 3, 64–69 (2009)
11. Ronsse, R., De Rossi, S., Vitiello, N., Lenzi, T., Carrozza, M.C., Ijspeert, A.J.: Real-Time Estimate of Velocity and Acceleration of Quasi-Periodic Signals Using Adaptive Oscillators. IEEE Transactions on Robotics 29, 783–791 (2013)
12. Righetti, L., Ijspeert, A.J.: Programmable central pattern generators: an application to biped locomotion control. In: IEEE International Conference on Robotics and Automation, ICRA, pp. 1585–1590 (2006)
13. Gams, A., Petric, T., Ude, A., Lajpah, L., Zaier, R.: Performing Periodic Tasks: On-Line Learning, Adaptation and Synchronization with External Signals. In: The Future of Humanoid Robots Research and Applications, pp. 3–28 (2012)
14. de Pina Filho, A.C., Dutra, M.S., Santos, L., Raptopoulos, C.: Modelling of Bipedal Robots Using Coupled Nonlinear Oscillators (2006)
15. Ronsse, R., Koopman, B., Vitiello, N., Lenzi, T., De Rossi, S.M.M., van den Kieboom, J., et al.: Oscillator-based walking assistance: A model-free approach. In: IEEE International Conference on Rehabilitation Robotics (ICORR), pp. 1–6 (2011)
16. Rinderknecht, M.D., Delaloye, F.A., Crespi, A., Ronsse, R., Ijspeert, A.J.: Assistance using adaptive oscillators: Robustness to errors in the identification of the limb parameters. In: IEEE International Conference on Rehabilitation Robotics (ICORR), pp. 1–6 (2011)
17. Swevers, J., Ganseman, C., Tukel, D.B., De Schutter, J., Van Brussel, H.: Optimal robot excitation and identification. IEEE Transactions on Robotics and Automation 13, 730–740 (1997)
18. Khalil, W., Dombre, E.: Modelisation, identification et commande des robots: Hermes science publ. (1999)